International Journal of Power Electronics and Drive System (IJPEDS)
Vol. 15, No. 2, June 2024, pp. 902∼912
ISSN: 2088-8694, DOI: 10.11591/ijpeds.v15.i2.pp902-912

Simulation and optimization of EMI filter of conducted emission for high voltage gain DC-DC converter

Abdelaali Ouhammam[1,2], Hassane Mahmoudi[1], Youssef El Hachimi[1,2], Amina Daghouri[2,3]
[1]EPTICAR Power Electronics Smart Techniques of Control, Automatics and Robotics Team, University Center for Research in Space Technologies, Mohammadia School of Engineers, Mohammed V University, Rabat, Morocco
[2]University Center for Research in Space Technologies, Mohammadia School of Engineers, Mohammed V University, Rabat, Morocco
[3]EODIC Energy Optimization, Diagnosis and Control Team, ENSAM, Mohammed V University, Rabat, Morocco

Article Info

Article history:

Received Jun 9, 2023
Revised Oct 30, 2023
Accepted Nov 7, 2023

Keywords:

CubeSat
Conducted emission
Electromagnetic compatibility
Electromagnetic interference filter
Optimization procedure

ABSTRACT

In the continuity of the work on design of high voltage gain DC-DC converter, used for feeding the CubeSat electrospray thrusters with a variable output voltage according to the maneuver size, this paper introduces a simulation of the converter model with MATLAB/Simulink to determine its conducted emission level. By referring to the MIL-STD-461 standard, a required passive electromagnetic interference (EMI) filter parameters are calculated to reduce, under thresholds, the converter noise. With consideration of the available volume and power constraints in this kind of satellite, the design of common-mode (CM) choke is optimized with proposed procedure optimization, so as to reduce its volume and electrical losses. Also, this optimization procedure can be generalized and applied for any passive EMI filter design.

This is an open access article under the CC BY-SA license.

Corresponding Author:

Abdelaali Ouhammam
EPTICAR Power Electronics Smart Techniques of Control, Automatics and Robotics Team
University Center for Research in Space Technologies, Mohammadia School of Engineers
Mohammed V University
Rabat, Morocco
Email: ouh.abdelaali@gmail.com

1. INTRODUCTION

For DC-DC converters, increasing the switching frequency of semiconductor switches can, significantly, reduce the size of passive components such as capacitors and coils. However, this high switching frequency generates signals with high $\frac{di}{dt}$ and $\frac{dv}{dt}$ causing conducted and radiated disturbances [1], [2], which are injected into the environment around the so-called "source" equipment, and impact the normal behavior of the so-called "victim" equipments sharing the same environment, and the generated noise is propagated under two modes: common mode (CM) and differential mode (DM). Their cancellation is impossible, though, there are some techniques that allow to attenuate their level to be under the limits defined in the electromagnetic compatibility (EMC) standards. In this sense, several solutions are proposed in the literature concerning the noise mitigation. First solution used is the passive electromagnetic interferences (EMI) filters [3], they reduce, considerably, the noise but their size and weight have a disadvantage limiting their usage for applications with constraints in available volume. In order to reduce the passive EMI filters dimensions, several papers introduce approaches that reduce the source noise. Among these strategies, there is printed circuit board (PCB) layout optimization [4], its goal is to reduce the inductance loop and parasitic capacitors. Another option concerns the modulation strategy where a random modulation presents improvement in EMI reduction compared to classical pulse width modulation [5]-[8]. As an alternative, there is the adoption of soft switching like a control approach [9], [10]. Second solution consists of the usage of active EMI filters [11]-[13], these kind of filters have reduced dimensions but they are more restrictive for the range of noise wider than their bandwidth. Finally, there is hybrid EMI filters [14], [15], which combine the passive filter used to attenuate the noise at high frequencies and the active filter to reduce the noise at low frequencies, therefore, the size and weight are reduced compared to conventional passive filters.

This article addresses electromagnetic interference generated by a high-voltage gain DC-DC converter used for feeding the CubeSats electrospray propulsion. This converter is intended to be operational within the space environment, therefore, and given the sensitivity of active filters to radiation due to the use of integrated circuits, only the passive EMI filter, which is composed with passive components, provides the filtering for the proposed DC-DC converter. In addition, this converter will be embedded in a CubeSat, which means other constraints to take into consideration, namely the available volume and the electrical energy generated on-board. Since the EMI filter occupies a significant part of the converter size, hence the need to reduce its size and increase its efficiency. Also, because the CM choke occupies a large space and consumes more electrical power in passive EMI filter, an optimization of its volume and its electrical losses is required. Some papers have already raised this type of optimization problem, in particular, [16]-[19] but without addressing the minimization of the filter electrical losses.

The optimization procedure adopted in this paper is based on the MATLAB function ”fmincon” and taking into account a number of constraints detailed in the next section. This optimization can be generalized and applied when designing passive EMI filters for converters intended to operate in an environment where both volume and electrical consumption constraints are imposed.

The equipment under test considered is a high voltage gain DC-DC converter used in electric propulsion for CubeSats [20], as shown in Figure 1, its characteristics are detailed in Table 1. Therefore, it is necessary to refer to the aerospace standards, especially the MIL-STD-461 standard, which generally defines the measurement setups of electromagnetic interferences and limit values not to be exceeded for equipment emissions and susceptibility.

The organization of this paper is delineated into 3 distinctive sections. Section 2 gives details about the simulation of conducted emissions generated by the proposed converter and provides a description of the optimization procedure for the design of the CM choke. The outcomes of this optimization are examined and discussed in section 3. The concluding remarks and perspectives of the present work in section 4.

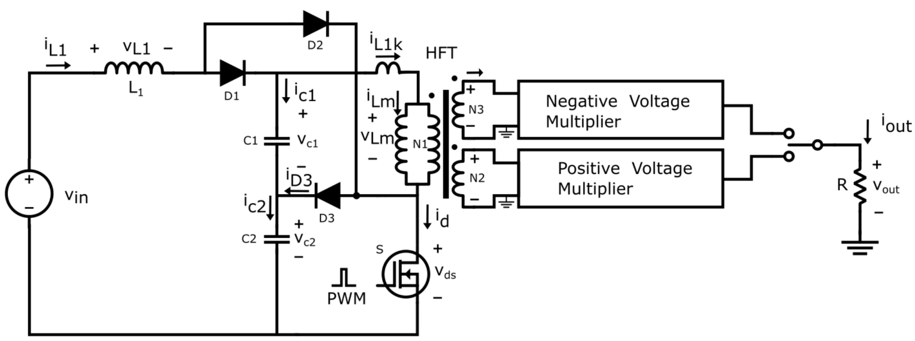

Figure 1. DC-DC converter topology

Table 1. Parameter and component values

Parameter	Value	Component	Size
Switching frequency F	100 kHz	L_1 and L_m	650 µH and 3.94 mH
Duty cycle D	57 - 70 %	c_1, c_2 and c_{vm}	1.72 µF, 1.1 µF and 10 nF
Transformer ratio N	6	D_1,D_2 and D_3	200V, 5 A
Multiplier voltage stage number n	4	D_{vm}	1 kV, 1 A
Load R	1 MΩ	Switch	200 V, 10 A, 0.06 Ω
Input voltage and output voltage	10 V and 1500 - 3500 V		

2. RESEARCH METHOD

2.1. Simulation of conducted emissions of the proposed converter

In this part, the measure of the converter's conducted emissions will be conducted through MATLAB simulations. The outcomes of these simulations will be compared against the established limits outlined in the MIL-STD-461 standard. The objective is to determine a required passive EMI filter parameters, which will then serve as input for the optimization procedure.

2.1.1. Description of simulation

The tool MATLAB/Simulink is used to simulate the conducted emission generated by the proposed converter, as outlined in Figure 2. To make the results of the simulation close to those of experimental, especially, for CM noise, parasitic capacitors are included in the model [21], namely, between load and ground, between primary and secondary of the transformer and between drain of the Mosfet and ground. In addition, the model of line impedance stabilization network (LISN) is placed between the device under test and the power source to block the passage of EMI between them, to stabilize the impedance of power source and to measure the conducted emission specific to the converter.

Once the steady state is established, the simulated spectrum of conducted emission injected by the proposed converter is visualized via the model of spectrum analyzer in Simulink. Because the measurements displayed on the spectrum are in dBm and the limits are in dBµV, the conversion from dBm to dBµV is necessary where dBµV = dBm + 107 (with the impedance equals 50 Ω). The power combiner, indicated in Figure 2, is used to separate the common mode and differential mode noises. Where $P_1 = (V_{DM} + V_{CM})^2/R_1$, represents the total conducted emission, and $P_2 = (V_{DM} - V_{CM})^2/(R_2 = R_1 = R)$, then $P_{DM} = V_{DM}^2/R = (P_1 + P_2)/4 + \sqrt{P_1 P_2}/2$ and $P_{CM} = V_{CM}^2/R = (P_1 + P_2)/4 - \sqrt{P_1 P_2}/2$.

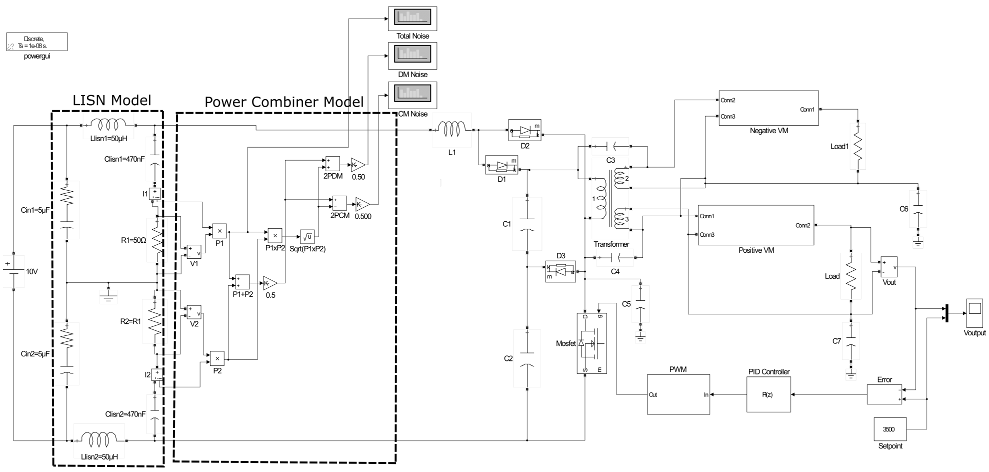

Figure 2. Conducted emissions simulation

2.1.2. Simulation results

Given that the proposed converter is designed for space applications and by referring to the requirement matrix described in the MIL-STD-461 standard, it can be seen that the CE102 (conducted emissions, radio frequency potential, power leads) requirement is applicable for DC source voltage of 28 V from 10 kHz to 10 MHz, in order to evaluate the level of conducted emission produced by this converter. Since this converter is designed to generate a variable output voltage within the range of 1500-3500 V, the simulation of conducted emissions has been conducted for two distinct setpoints: 1500 V and 3500 V, as depicted in Figure 3. The subsequent sections will focus on the case with a setpoint of 3500 V, as it represents the worst-case scenario in terms of the level of conducted emissions.

Before starting the design of EMI filter parameters, it is necessary to separate the DM noise from CM noise to get an idea about the contribution of each mode in the total EMI noise generated and to make the filter design more judicious. From Figure 4(a) and 4(b), it can be seen that the level of conducted emission for DM and CM exceeds, respectively, the CE102 thresholds with 40 dBμV. To comply with EMC standards, the designed EMI filter shall achieve an attenuation higher than 40 dBμv.

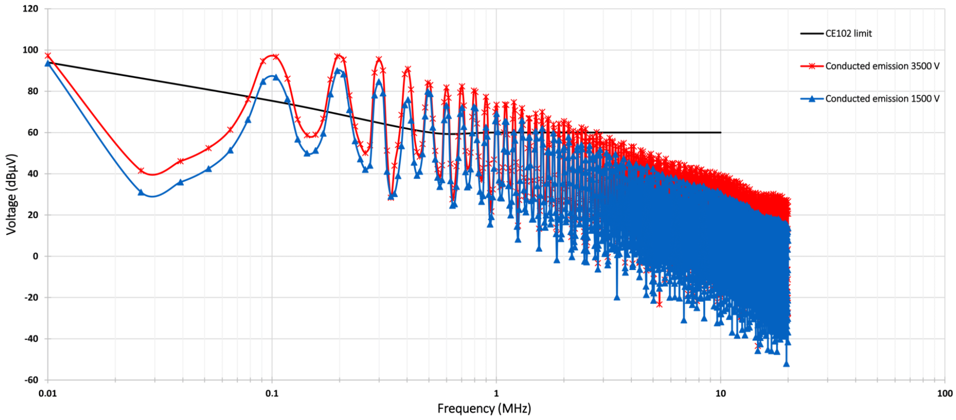

Figure 3. Total conducted emission of the proposed converter without EMI filter

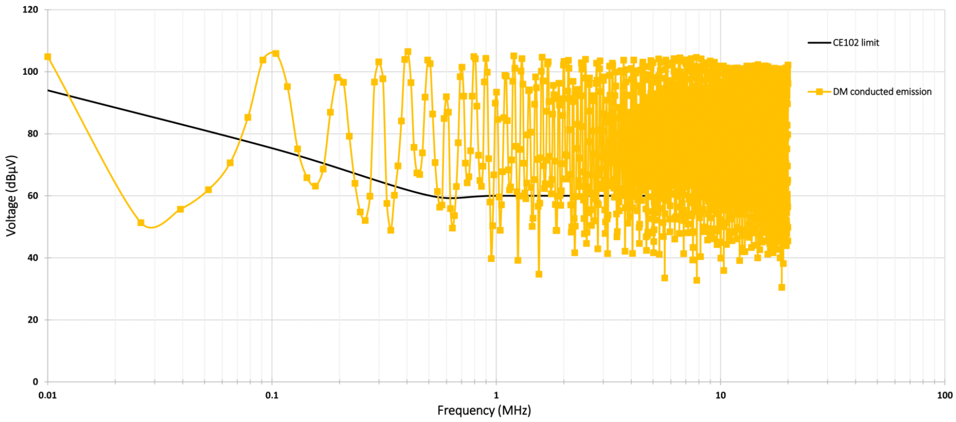

(a)

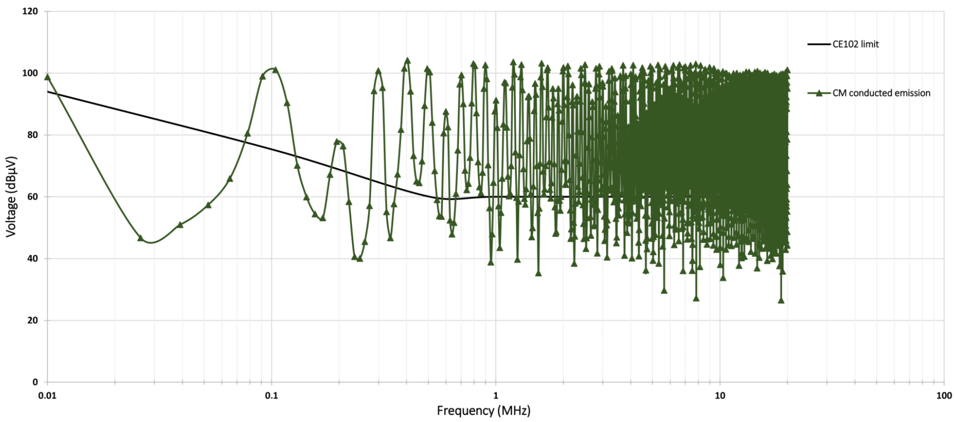

(b)

Figure 4. Conducted emission of the proposed converter without EMI filter for (a) DM and (b) CM

2.1.3. Determination of required passive EMI filter parameters

Meet CE regulations of MIL-STD-461 is the purpose of the EMI filter, it attenuates the amplitudes of conducted emissions (CM and DM) under the CE102 limits with a margin at least of 6 dB to account for simulation deviations and to ensure sufficient margin under of the EMC standard for the frequency range. Using (1) and (2) detailed in [22] to calculate the required EMI filter parameters, which will be used as inputs for optimization procedure.

– For DM part: this mode is dominant in the low frequencies around switching frequency 100 kHz, thus, the cutoff frequency of the DM EMI filter must be equal to f_{Rdm} =10kHz, to ensure an attenuation of 40 dBμV, as shown in Figure 4(a).

$$L_{dmreq} = \frac{1}{C_x(2\pi f_{Rdm})^2} \quad (1)$$

Where $C_{x1} = C_{x2} = C_x$= 22 μF thus L_{dmreq}= 11.5 μH.

– For CM component: this mode is dominant in the high frequencies around 1 MHz because the parasitic capacitances are very low. To have an attenuation of 40 dBμV, as indicated in Figure 4(b), with a slope of -40 dB/decade, the cutoff frequency of the CM EMI filter shall be f_{Rcm} =100 kHz.

$$L_{cmreq} = \frac{1}{2C_y(2\pi f_{Rcm})^2} \quad (2)$$

Where C_y= 5 nF thus L_{cmreq}= 253.5 μH.

Figure 5 shows the synoptic of the passive EMI filter to be designed, and to reduce the size of EMI filter, the leakage inductance L_{lk} of CM choke coil will be used as DM inductor.

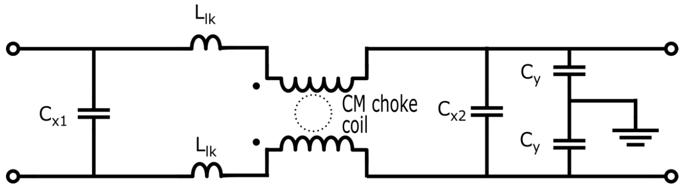

Figure 5. Synoptic of passive EMI filter

2.2. Optimization procedure of CM choke design

An optimization of the volume and losses of the CM choke allows to reduce the size of the converter breadboard and increase its electrical efficiency. Therefore, this board will be more adapted to the volume and consumption constraints imposed by the CubeSats on all on-board subsystems. This part will be devoted to CM choke optimization procedure by detailing the involved constraints and the followed algorithm.

2.2.1. List of constraints

The choice of the CM choke parameters indicated in Figure 6, namely, the dimensions of the magnetic core (x(1)=OD, x(2)=ID, x(3)=H), the winding turns number (N=x(4)) and the angle occupied by the coil on the core (x(5)=θ), is optimized in order to reduce the volume and losses of the CM choke by taking several constraints (mechanical, magnetic and electrical) into account for the correct operation of the filter.

– Inductance constraints: To mitigate the CM EMI noise, it is imperative that the CM inductance surpasses the specified threshold denoted as L_{cmreq}, as mentioned in (3). Adhering to this criterion ensures that the CM inductance is appropriately dimensioned to address the targeted CM EMI noise, contributing to enhanced overall system performance and electromagnetic compatibility.

$$L_{cmreq} \leq L_{cm} = \mu_0 \mu_r \frac{N^2 A_e}{l_e} \quad (3)$$

Where μ_0 is the Vacuum permeability, μ_r is The relative permeability for a core material, A_e=$x(3)(x(1) - x(2))/2$ is the effective cross sectional area of the core and l_e=$2\pi(x(1) + x(2))/4$ is the

effective length of the magnetic path of the core.
DM Inductance which equals Leakages inductance of CM choke [23], shall be greater than L_{dmreq}, as expressed in (4), to filter the part of DM EMI noise.

$$L_{dmreq} \leq L_{dm} = L_{lk} \approx 2.5\mu_0 \frac{N^2 A_e}{l_e\sqrt{\theta/(2\pi) + sin(\theta/2)/\pi}} (\sqrt{\pi/A_e} l_e/2)^{1.45} \tag{4}$$

– Core saturation constraint: Preventing core saturation necessitates that the magnetic flux density, denoted as B_{pk}, generated by common-mode and differential-mode currents, remains below the saturation flux density of the core, denoted as B_{sat}, as outlined in (5) [24]. Given the low values of L_{lk} and I_{cmpk}, this constraint is typically guaranteed, ensuring the effective avoidance of core saturation.

$$B_{pk} = \frac{L_{cm} I_{cmpk} + L_{lk}(I_{cmpk} + I_{dmpk})}{2NA_e} \leq B_{sat} \tag{5}$$

Where I_{cmpk} is the peak CM current and I_{dmpk} is the peak DM current.

– Core dimensions constraint: In order to accommodate the inductance windings, it is imperative that the inner radius of the core exceeds the minimum specified value $R_{\text{min}} = \frac{2Nd^2}{ID\theta}$, as mentioned in (6), that represents the necessary thickness of the winding wire around the core. Adhering to this criterion ensures proper spatial allocation for the inductance windings.

$$ID \geq 2d\sqrt{N/\theta} \tag{6}$$

Where d is the winding wire diameter.

– Stability constraint: Applying the Middlebrook criterion [25] is essential for securing the stability of the proposed DC-DC converter. According to this criterion, it is imperative that the output impedance of the filter, denoted as Z_{out}, consistently maintains a value lower than the input impedance of the converter, represented by Z_{in}, as described by (7).

$$Z_{out} = \sqrt{L_{lkmax}/C_x} \leq Z_{in} = \frac{v_{in}^2 R\eta}{2v_{out}^2} \tag{7}$$

Where η is the efficiency of proposed converter.

2.2.2. Optimization design algorithm

The objective function to be minimized combines volume and electrical losses with weighted coefficients, as detailed in (8). The "**fmincon**" of MATLAB is used as a nonlinear programming solver to find the minimum of the objective function, then after a number of iterations, its optimization algorithm "**interior-point**" converges to an optimal choice of the five parameters (OD, ID, H, N and θ) related to CM choke.

$$Obj - Fun = w_1.Vol(x) + w_2.Los(x) \tag{8}$$

Where $Vol(x) = \pi(\frac{x(1)}{2} + \frac{4x(4)d^2}{(x(1)+x(2))x(5)})^2(x(3) + \frac{8x(4)d^2}{(x(1)+x(2))x(5)})$ assuming that $\frac{(x(1)+x(2))x(5)}{4} - dx(4) \leq 0$ and $Los(x)$ =Winding loss+Core loss= $\frac{8\rho(x(3)+x(1)-x(2))x(4)I^2}{d^2}$+$8F^{1.621}(\frac{(L_{cm}+L_{lk})I_{cmpk}}{(x(1)-x(2))x(3)x(4)})^{1.982}$ $pi(x(1)^2 - x(2)^2)x(3)/4$ [26] with I is the input current of converter and ρ is the resistivity of copper.

Figure 7 encapsulates the methodology of the common-mode (CM) choke design optimization algorithm through a concise flow chart. The process is initiated by defining a set of inputs, followed by the imposition of constraints integral to the design optimization. As for the dimensions of the magnetic core, there are two cases; Choosing the standard dimensions which are close to optimal dimensions proposed by this algorithm, or it is possible to order the magnetic cores with the specific dimensions directly from the manufacturer.

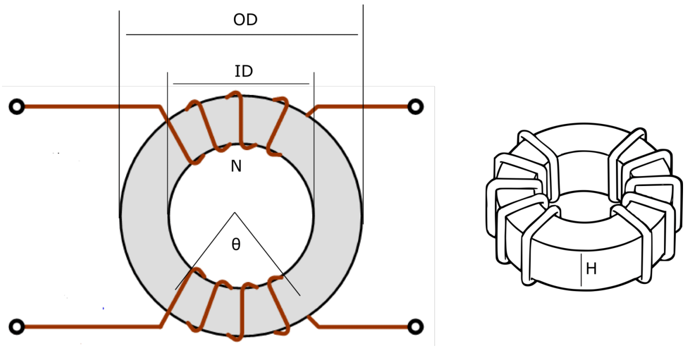

Figure 6. CM choke parameters

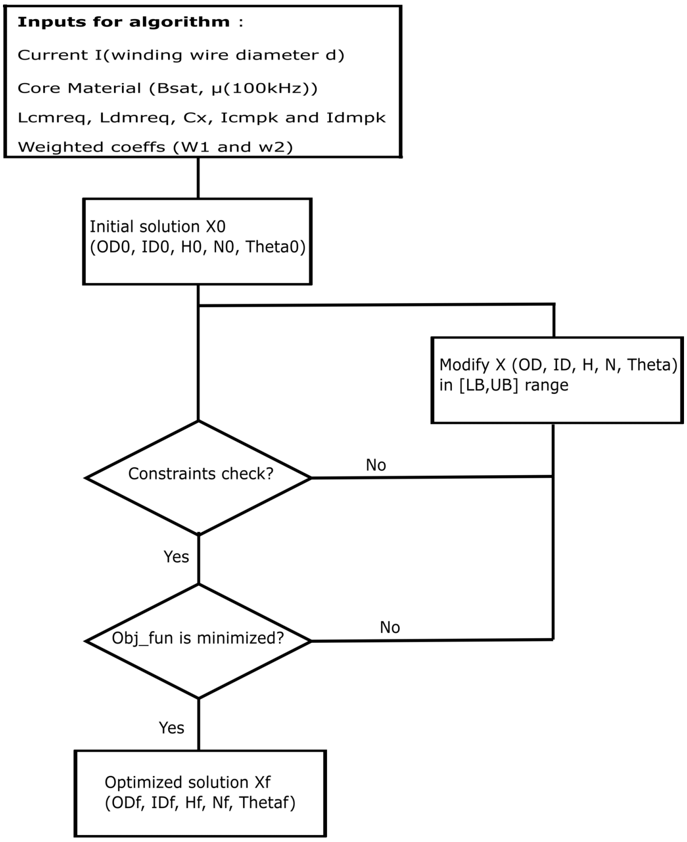

Figure 7. Optimization algorithm flow chart

3. OPTIMIZATION RESULTS AND DISCUSSION

The optimization algorithm, outlined above, is implemented in MATLAB, selecting the optimal parameters for the CM choke based on the inputs specified in Table 2. In this context, nanocrystalline is chosen as the core material, and the values of I_{cmpk} and I_{dmpk} are computed in accordance with the CE102 standard. The algorithm successfully converges after 25 iterations, yielding an objective function value of 1.15, as visually depicted in Figure 8. This outcome represents the minimum achieved while adhering to all the constraints described earlier.

To assess the incremental value of the optimization procedure, a thorough comparison is conducted between the results of an intuitive design, which meets all the specified constraints without optimization, and the outcomes derived from the proposed optimization procedure. Table 3 compiles essential metrics such as CM choke volume, CM choke electrical losses, dimensions of the magnetic core, and winding parameters for each design approach. Notably, the optimized results exhibit a considerable reduction compared to the intuitive design outcomes. The optimization procedure demonstrates a gain exceeding 10 for the CM choke volume, and there is a notable reduction of more than 30% in electrical losses. These results underscore the substantial improvement achieved through the optimization process.

Table 2. Algorithm input parameters

Parameter	Value
Input current I	3 A
Winding wire diameter d	1 mm
L_{cmreq}, L_{dmreq} and C_x	253.5 μH,11.5 μH and 22 μF
Weighted coefficients w_1=w_2	0.5
I_{cmpk}=I_{dmpk}	0.06 Arms
B_{sat} and $\mu_r(100kHz)$	1.25 T and 20000
Lower Bounds LB	[1.12, 0.51, 0.58, 1, $\pi/3$]
Upper Bounds UB	[16.69, 12.39, 3.05, 100, π]

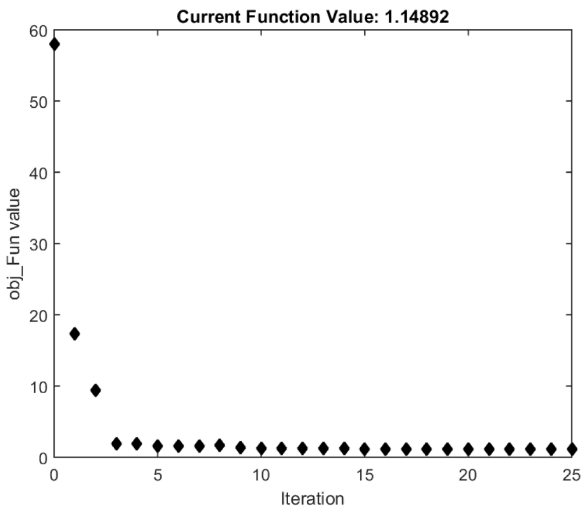

Figure 8. Obj-Fun values

Table 3. Comparison results

	$Vol(cm^3)$	Los (W)	OD (cm)	ID (cm)	H (cm)	N (turn)	θ (rad)
Intuitive design	21.83	0.29	3.46	1.73	1.73	14	1.05
Proposed design	2.08	0.22	1.20	0.62	0.58	31	π

Also, on the catalogs offered in the market, the standard magnetic core W902 with dimensions 1.41x0.66x0.63 (cmxcmxcm) close to the output of the algorithm.Using these five parameters, the calculated CM choke inductances are L_{cm}=13.6 mH and L_{lk}=11.5 μH. To visualize the impact of passive EMI filter on conducted emission of proposed converter, a simulation is performed with the implementation of the filter components in the Simulink model between the LISN and the converter, L_{cm}=13.6 mH, L_{lk}=11.5 μH, C_x=22 μF and C_y=5 nF. In Figure 9, it can be noticed that the conducted emission level is attenuated with a sufficient margin below CE102 limits. Only for the second harmonic (F=200kHz), where the margin of 3 dB under the limits is low compared to those of the other harmonics.

As mentioned in introduction, this optimization procedure can be generalized and used, for other converter with different input power, as guideline for a choice of the magnetic core and winding parameters.

Table 4 summarizes the five parameters optimization for different winding wire diameters dependent on the input current. For an input current,assuming that the required inductances are the same, the core dimensions calculated allow to choose, easily, the appropriate core on catalog with reducing the occupied volume and electrical losses by satisfying the attenuation requirement.

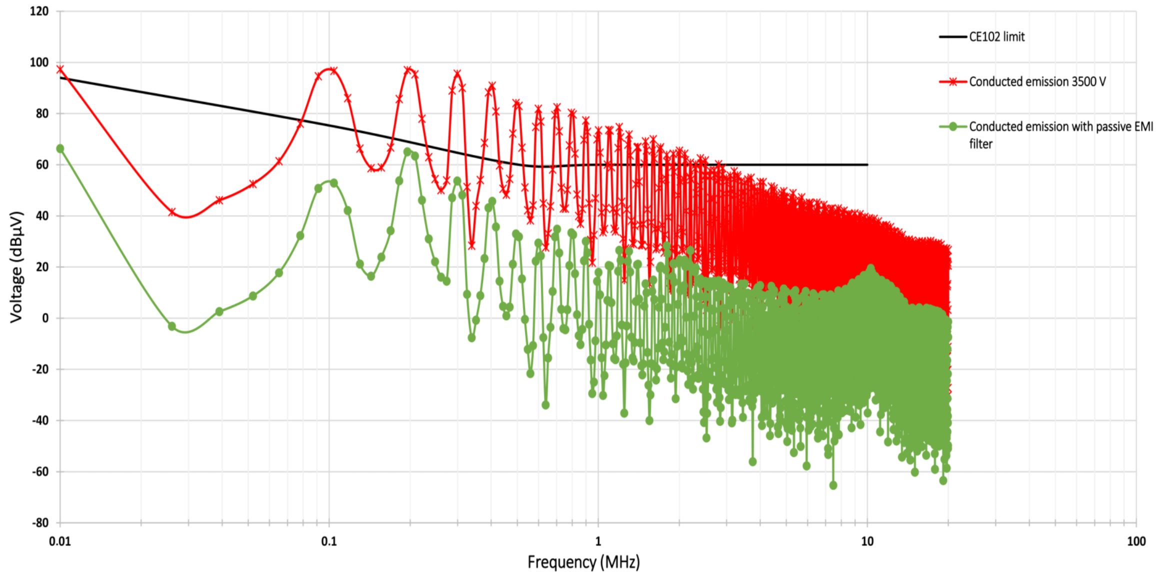

Figure 9. Total conducted emission of the proposed converter with EMI filter

Table 4. Optimization results for different winding wire diameters

d(cm)	$Vol_{min}(cm^3)$	Los_{min} (W)	OD (cm)	ID (cm)	H (cm)	N (turn)	θ (rad)
0.05	0.84	0.10	1.12	0.58	0.58	32	π
0.10	2.08	0.22	1.20	0.62	0.58	31	π
0.15	5.26	0.28	1.54	0.94	0.60	31	π
0.20	10.48	0.46	1.94	1.18	0.76	28	π
0.25	17.91	0.50	2.33	1.41	0.92	25	π

4. CONCLUSION

In this paper, the conducted emission generated by the proposed converter is simulated in MATLAB/Simulink . Due to the sensitivity of integrated circuits to radiation in space, the passive EMI filter ensures the filtering operation alone. In addition, the proposed optimization procedure is used to minimize the volume and electrical losses of CM choke, also can be applied for any passive EMI filter design, by acting on the core dimensions, the winding turns number and the angle occupied by the coil. Then the effectiveness of the proposed filter is verified by Simulink simulations. As a perspective for this paper, it is planned to perform the experimental prototype of the proposed filter and to check its effectiveness in conducted emission mitigation.

ACKNOWLEDGEMENTS

This work has been performed within the framework of the “University Nanosatellites” project between Mohammed V University (UM5R) and the Royal Center for Space Studies and Research (CRERS), Morocco.

REFERENCES

[1] X. Pei, J. Xiong, Y. Kang, and J. Chen, “Analysis and suppression of conducted EMI emission in PWM inverter,” in *IEMDC 2003 - IEEE International Electric Machines and Drives Conference*, 2003, vol. 3, pp. 1787–1792, doi: 10.1109/IEMDC.2003.1210695.

[2] T. Ninomiya, M. Shoyama, C. F. Jin, and G. Li, "EMI issues in switching power converters," in *IEEE International Symposium on Power Semiconductor Devices and ICs (ISPSD)*, 2001, pp. 81–85, doi: 10.1109/ispsd.2001.934563.

[3] J. L. Kotny, T. Duquesne, and N. Idir, "Design of EMI filters for DC-DC converter," in *2010 IEEE Vehicle Power and Propulsion Conference, VPPC 2010*, Sep. 2010, pp. 1–6, doi: 10.1109/VPPC.2010.5729047.

[4] A. Bhargava, D. Pommerenke, K. W. Kam, F. Centola, and C. W. Lam, "DC-DC buck converter EMI reduction using PCB layout modification," *IEEE Transactions on Electromagnetic Compatibility*, vol. 53, no. 3, pp. 806–813, Aug. 2011, doi: 10.1109/TEMC.2011.2145421.

[5] F. Mihalič and D. Kos, "Reduced conductive EMI in switched-mode dc-dc power converters without EMI filters: PWM versus randomized PWM," *IEEE Transactions on Power Electronics*, vol. 21, no. 6, pp. 1783–1794, Nov. 2006, doi: 10.1109/TPEL.2006.882910.

[6] G. M. Dousoky, M. Shoyama, and T. Ninomiya, "Conducted-noise characteristics of a digitally-controlled randomly-switched dc-dc converter with an FPGA-based implementation," *Journal of Power Electronics*, vol. 10, no. 3, pp. 228–234, May 2010, doi: 10.6113/JPE.2010.10.3.228.

[7] H. Li, Y. Ding, Z. Yang, and Y. Jiang, "Optimization design of EMI filter with chaotic PWM in DC-DC converters," in *WiPDA Asia 2019 - IEEE Workshop on Wide Bandgap Power Devices and Applications in Asia*, May 2019, pp. 1–6, doi: 10.1109/WiPDAAsia.2019.8760318.

[8] K. Cui, V. Adrian, B. H. Gwee, and J. S. Chang, "A noise-shaped randomized modulation for switched-mode DC-DC converters," *IEEE Transactions on Circuits and Systems I: Regular Papers*, vol. 65, no. 1, pp. 394–405, Jan. 2018, doi: 10.1109/TCSI.2017.2719700.

[9] N. Sudhakar, N. Rajasekar, V. T. Rohit, E. Rakesh, and J. Jacob, "EMI mitigation in closed loop boost converter using soft switching combined with chaotic mapping," in *2014 International Conference on Advances in Electrical Engineering, ICAEE 2014*, Jan. 2014, pp. 1–6, doi: 10.1109/ICAEE.2014.6838488.

[10] M. Khodabandeh, E. Afshari, and M. Amirabadi, "A family of ĆUK, Zeta, and SEPIC based soft-switching DC-DC converters," *IEEE Transactions on Power Electronics*, vol. 34, no. 10, pp. 9503–9519, Oct. 2019, doi: 10.1109/TPEL.2019.2891563.

[11] D. Hamza and P. K. Jain, "Conducted EMI noise mitigation in DC-DC converters using active filtering method," in *PESC Record - IEEE Annual Power Electronics Specialists Conference*, Jun. 2008, pp. 188–194, doi: 10.1109/PESC.2008.4591923.

[12] Y. Zhou *et al.*, "A new integrated active EMI filter topology with both CM noise and DM noise attenuation," *IEEE Transactions on Power Electronics*, vol. 37, no. 5, pp. 5466–5478, May 2022, doi: 10.1109/TPEL.2021.3130113.

[13] J. Ramakrishnan and C. N. Ravi, "Optimization of passive filter components through active filtering of current ripple reduction in an inverter," *International Journal of Power Electronics and Drive Systems (IJPEDS)*, vol. 13, no. 1, pp. 298–308, Mar. 2022, doi: 10.11591/ijpeds.v13.i1.pp298-308.

[14] J. Biela, R. Waespe, K. Raggl, J. W. Kolar, A. Wirthmueller, and M. L. Heldwein, "Passive and active hybrid integrated EMI filters," *IEEE Transactions on Power Electronics*, vol. 24, no. 5, pp. 1340–1349, May 2009, doi: 10.1109/TPEL.2009.2012404.

[15] M. Ali, E. Labouré, F. Costa, and B. Revol, "Design of a hybrid integrated EMC filter for a DC-DC power converter," *IEEE Transactions on Power Electronics*, vol. 27, no. 11, pp. 4380–4390, Nov. 2012, doi: 10.1109/TPEL.2012.2183387.

[16] S. Khelladi, K. Saci, A. Hadjadj, and A. Ales, "A hybrid common mode choke optimization method for input line emi filter design," *Advanced Electromagnetics*, vol. 10, no. 2, pp. 56–66, Jul. 2021, doi: 10.7716/aem.v10i2.1677.

[17] B. Zaidi, A. Videt, and N. Idir, "Optimization method of CM inductor volume taking into account the magnetic core saturation issues," *IEEE Transactions on Power Electronics*, vol. 34, no. 5, pp. 4279–4291, May 2019, doi: 10.1109/TPEL.2018.2861620.

[18] X. Zhao, J. Hu, L. Ravi, D. Dong, and R. Burgos, "Planar common-mode EMI filter design and optimization in a 100-kW SiC-based generator-rectifier system for high-altitude operation," in *2021 IEEE Energy Conversion Congress and Exposition, ECCE 2021 - Proceedings*, Oct. 2021, pp. 3555–3562, doi: 10.1109/ECCE47101.2021.9595304.

[19] S. Dey, A. Mallik, and S. Mishra, "A mathematical design approach to volumetric optimization of EMI filter and modeling of CM noise sources in a three-phase PFC," *IEEE Transactions on Power Electronics*, vol. 37, no. 1, pp. 462–472, Jan. 2022, doi: 10.1109/TPEL.2021.3097963.

[20] A. Ouhammam, H. Mahmoudi, and H. Ouadi, "Design and control of high voltage gain DC–DC converter for CubeSat propulsion," *CEAS Space Journal*, Apr. 2023, doi: 10.1007/s12567-023-00493-0.

[21] L. Zhai, G. Hu, M. Lv, T. Zhang, and R. Hou, "Comparison of two design methods of EMI filter for high voltage power supply in DC-DC converter of electric vehicle," *IEEE Access*, vol. 8, pp. 66564–66577, 2020, doi: 10.1109/ACCESS.2020.2985528.

[22] Nidhal Y. Nasser, "Practical approach in designing conducted EMI filter to mitigate common mode and differential mode noises in SMPS," *Journal of Engineering an d Development*, vol. 16, no. 1, pp. 164–183, 2012, [Online]. Available: http://www.iasj.net/.

[23] M. L. Heldwein, L. Dalessandro, and J. W. Kolar, "The three-phase common-mode inductor: Modeling and design issues," *IEEE Transactions on Industrial Electronics*, vol. 58, no. 8, pp. 3264–3274, Aug. 2011, doi: 10.1109/TIE.2010.2089949.

[24] D. Han, C. T. Morris, W. Lee, and B. Sarlioglu, "Three-phase common mode inductor design and size minimization," in *2016 IEEE Transportation Electrification Conference and Expo, ITEC 2016*, Jun. 2016, pp. 1–8, doi: 10.1109/ITEC.2016.7520267.

[25] R. D. Middlebrook and S. Cuk, "A general unified approach to modelling switching-converter power stages," in *1976 IEEE Power Electronics Specialists Conference*, Jun. 2015, pp. 18–34, doi: 10.1109/pesc.1976.7072895.

[26] W. Shen, F. Wang, D. Boroyevich, and C. W. Tipton, "Loss characterization and calculation of nanocrystalline cores for high-frequency magnetics applications," in *Conference Proceedings - IEEE Applied Power Electronics Conference and Exposition - APEC*, Feb. 2007, pp. 90–96, doi: 10.1109/APEX.2007.357500.

BIOGRAPHIES OF AUTHORS

Abdelaali Ouhammam received the Engineer degree in Electro-techanical and Power Electronics, in 2014, from Mohammadia School of Engineers-Rabat, Morocco. He is currently Ph.D. student in Aerospace Engineering at the University Center for Research in Space Technologies of Mohammadia School of Engineers. His research interests include the field of power electronics and electromagnetic compatibility. He can be contacted at email: ouh.abdelaali@gmail.com.

Hassane Mahmoudi received B.S degree in electrical engineering from Mohammadia School of Engineers, Rabat, Morocco, in 1982, and the Ph.D. degree in power electronic from Montefiore Institute of Electrical Engineering, Luik, Belgium, in 1990. He was an assistant professor of physics, at the Faculty of Sciences, Meknes, Morocco, from 1982 to 1990. Since 1992, he has been a professor at the Mohammadia Schools of Engineers, Rabat, Morocco. He was the head of electric engineering department during four years (1999, 2000, 2006 and 2007), and the Deputy Director in charge of Research and Cooperation between 2019 and 2022. Since 2022, he has held the director position of Mohammadia School of Engineers. His research interests include static converters, electrical motor drives, active power filters, and the compatibility electromagnetic. He can be contacted at email: mahmoudi@emi.ac.ma.

Youssef El Hachimi received the Engineer degree in Electronic and Automatic Systems, in 2021, from National School of Applied Sciences-Tangier, Morocco. He is working toward the Ph.D. degree in Electrical Engineering and Space Technologies at the University Center for Research in Space Technologies of Mohammadia School of Engineers. His research interests include the electrical power systems, and electromagnetic compatibility in aerospace systems. He can be contacted at email:youssef.elhachimi@research.emi.ac.ma.

Amina Daghouri is an IEEE member and a Ph.D. student in Electrical Engineering at ENSAM Rabat, Mohammed V University in Rabat. She received her Engineering Degree in Electrical Engineering from ENSET Rabat, Mohammed V University, Rabat, Morocco, in 2018. Embedded systems, hardware and software design, solar energy harvesting devices, energy storage, robust control, and nanosatellite electrical power systems are some of her research interests. She can be contacted at email: amina_daghouri@um5.ac.ma.